









Let I and II be two different world coordinate systems, the transition matrix between them be

$$\mathbf{G} = \begin{bmatrix} \mathbf{R} & \mathbf{t} \\ \mathbf{0} & \mathbf{1} \end{bmatrix}. \text{ In world coordinate system I, } \mathbf{M} \text{ is the coordinates of the 3D-point, } \mathbf{O}_i \text{ and } \mathbf{O}_j$$

are the homogeneous coordinates of optical centers of cameras  $i$  and  $j$ ,  $\mathbf{H}_i$  and  $\mathbf{H}_j$  are the projection matrix of cameras  $i$  and  $j$ . In similar way, we can denote  $\mathbf{M}'$ ,  $\mathbf{O}_i'$  and  $\mathbf{O}_j'$ ,  $\mathbf{H}_i'$  and  $\mathbf{H}_j'$  in II. Obviously, there are some the relationships as follow.

$$\mathbf{H}_i' = \mathbf{H}_i \mathbf{G} \quad (4)$$

$$\mathbf{H}_j' = \mathbf{H}_j \mathbf{G} \quad (5)$$

$$\mathbf{O}_i' = \mathbf{G}^{-1} \mathbf{O}_i \quad (6)$$

The fundamental matrix in world coordinate system I can be obtained as follows [16].

$$F = \begin{bmatrix} \mathbf{H}_j & \mathbf{O}_j \end{bmatrix}_X \mathbf{H}_i^+ \quad (7)$$

where  $\begin{bmatrix} \mathbf{H}_j \mathbf{O}_j \end{bmatrix}_X$  is a real skew-symmetric matrix constructed by vector  $\mathbf{H}_j \mathbf{O}_j$ ,  $\mathbf{H}_i^+$  is the pseudo-inverse matrix of  $\mathbf{H}_i$ .

According to Equation (4) ~ (7), the relationship between two fundamental matrixes in coordinate systems I and II is as follows.

$$F' = \begin{bmatrix} \mathbf{H}_j' \mathbf{O}_j' \end{bmatrix}_X \mathbf{H}_i' (\mathbf{H}_i')^+ = \begin{bmatrix} \mathbf{H}_j \mathbf{G} \mathbf{G}^{-1} \mathbf{O}_j \end{bmatrix}_X \mathbf{H}_j \mathbf{G} \mathbf{G}^{-1} \mathbf{H}_i^+ = \begin{bmatrix} \mathbf{H}_j \mathbf{O}_j \end{bmatrix}_X \mathbf{H}_i \mathbf{H}_i^+ = F \quad (8)$$

Equation (8) shows explicitly that for a fixed binocular system, the fundamental matrix is same in different world coordinate systems. This means that an invertible matrix  $\mathbf{G}$  cannot change the

value of the fundamental matrix. Following this way, we set  $\mathbf{G} = \begin{bmatrix} R & t \\ \mathbf{0} & \mathbf{1} \end{bmatrix}^{-1}$ , then

$$\mathbf{H}_i' = \mathbf{H}_i \mathbf{G} = [A_i, 0] \quad (9)$$

$$\mathbf{H}_j' = \mathbf{H}_j \mathbf{G} = \begin{bmatrix} A_j & \mathbf{0} \end{bmatrix} \begin{bmatrix} R_j & \mathbf{t}_j \\ \mathbf{0} & \mathbf{1} \end{bmatrix} \begin{bmatrix} R_i & t_i \\ \mathbf{0} & \mathbf{1} \end{bmatrix}^{-1} = \begin{bmatrix} A_j R_j R_i^T & A_j (t_j - R_j R_i^T t_i) \end{bmatrix} \quad (10)$$

$$\mathbf{O}_i' = \mathbf{G}^{-1} \mathbf{O}_i = 0, 0, 0, 1^T \quad (11)$$

$\mathbf{H}_j' \mathbf{O}_i'$  and  $\mathbf{H}_j' (\mathbf{H}_i')^+$  can be calculated by Equation (9) ~ (11),

$$\mathbf{H}_j' \mathbf{O}_i' = A_j (t_j - R_j R_i^T t_i) \quad (12)$$

$$\begin{aligned} \mathbf{H}_j'(\mathbf{H}_i')^+ &= \begin{bmatrix} A_j R_j R_i^T & A_j(t_j - R_j R_i^T t_i) \end{bmatrix} [A_i, 0]^+ \\ &= \begin{bmatrix} A_j R_j R_i^T & A_j(t_j - R_j R_i^T t_i) \end{bmatrix} \begin{bmatrix} A_i^{-1} \\ 0 \end{bmatrix} = A_j R_j R_i^T A_i^{-1} \end{aligned} \quad (13)$$

The new form of fundamental matrix, which is directly defined by the parameters of a cameras, can be achieved by substituting the results of Equation (12) and (13) in Equation (7) as follows.

$$F = [A_j(t_j - R_j R_i^T t_i)]_x A_j R_j R_i^T A_i^{-1} \quad (14)$$

Using the characteristic of real skew-symmetric matrix [16], another form of fundamental matrix can be obtained as follow.

$$\begin{aligned} F &= [A_j(t_j - R_j R_i^T t_i)]_x A_j R_j R_i^T A_i^{-1} \\ &= [A_j R_j (R_j^T t_j - R_i^T t_i)]_x A_j R_j R_i^T A_i^{-1} \\ &= (A_j R_j)^{-T} [(R_j^T t_j - R_i^T t_i)]_x R_i^T A_i^{-1} \end{aligned} \quad (15)$$

According to Equation (15), the epipolar constraint can be rewritten as follows.

$$\begin{aligned} m_j^T F m_i &= m_j^T (A_j R_j)^{-T} [(R_j^T t_j - R_i^T t_i)]_x R_i^T A_i^{-1} m_i \\ &= R_j^T A_j^{-1} m_j^T [(R_j^T t_j - R_i^T t_i)]_x R_i^T A_i^{-1} m_i = 0 \end{aligned} \quad (16)$$

Based on Fig. 1 and Equation (2), in world coordinate system I,  $-R_i^T t_i$  and  $-R_j^T t_j$  are the coordinates of the optical center,  $f_i \cdot R_i^T A_i^{-1} m_i$  is the direction vector of BPL emitted from camera I,  $f_j \cdot R_j^T A_j^{-1} m_j$  is the direction vector of BPL from camera II. Thus, the epipolar constraint can be described by BPL model.

$$m_j^T F m_i = \frac{1}{f_i f_j} L_j \cdot (S_i - S_j) \times L_i = 0 \quad (17)$$

It is notable that  $S_i - S_j$  is the baseline of the binocular system that is constructed by cameras  $i$  and  $j$ , additionally,  $L_i$  and  $L_j$  are the direction vectors of BPL.

It can be seen that Equation (17) is the signed volume of the parallelepiped defined by the three vectors. If the volume is equal to zero, the three vectors are coplanar. In other words, epipolar constraint finds corresponding points in a binocular system by validating whether two projective points and the baseline are coplanar. This is the geometric meanings of epipolar constraint, which is demonstrated as follows..

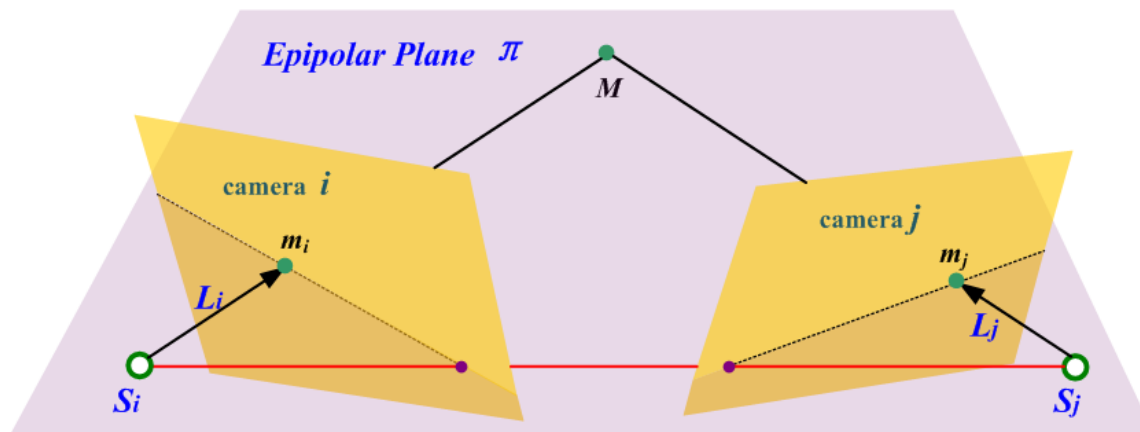


Figure. 2. The physical meaning of epipolar constraint

In Fig. 2, the binocular system has two cameras  $i$  and  $j$ , their optical central are  $S_i$  and  $S_j$ ,  $S_i - S_j$  is the baseline of the binocular system,  $m_i$  and  $m_j$  are the projection of a 3D-point on epipolar plane  $\pi$ , the direction vector of their BPL are  $L_i$  and  $L_j$ . If  $m_i$  and  $m_j$  are correspondence point,  $m_i$ ,  $m_j$ ,  $S_i$  and  $S_j$  are coplanar, and three vector  $L_i$ ,  $L_j$  and  $S_i - S_j$  are coplanar.

### c. The Analyses of Existing Methods

MP, ED, IA are point correspondence methods based on epipolar constraint, their geometric meanings are described by the mathematical expressions as follow.

$$MP = |m_j^T F m_i| = |L_j \cdot (S_i - S_j) \times L_i| < \theta \quad (18)$$

$$ED = \frac{|m_j F m_i|}{\sqrt{F_1^2 + F_2^2}} + \frac{|m_i F m_j|}{\sqrt{G_1^2 + G_2^2}} < \theta \quad (19)$$

$$IA = \frac{|[(S_i - S_j) \times L_i] \cdot [(S_i - S_j) \times L_j]|}{\|[(S_i - S_j) \times L_i]\| \|[(S_i - S_j) \times L_j]\|} < \theta \quad (20)$$

where  $(F_1, F_2, F_3)^T = F m_i$ ,  $(G_1, G_2, G_3)^T = F m_j$ ,  $\theta$  is a threshold. If their values are smaller than  $\theta$ , these method deem that these two projective points are corresponding.

MP method computes the volume of the parallelepiped which determined by three vectors,  $S_i - S_j$ ,  $L_i$  and  $L_j$ . In the most cases, the magnitude of  $S_i - S_j$  (baseline) is far greater than  $L_i$  and  $L_j$ , this means the value of MP mainly depends on the baseline of binocular system. For ED

method,  $Fm_i$  and  $Fm_j$  are polar lines, the value of ED is the sum of the distance from them to  $m_i$  and  $m_j$ . IA is the included angle between two collinear epipolar that are passing through the baseline and whose normal line are  $(S_i - S_j) \times L_i$  and  $(S_i - S_j) \times L_j$ .

It can be found that the parameters of cameras have influence on the values of these methods above. This means a binocular system requires a special threshold. Especially, for a multi-ocular system that can compose several binocular systems, there are several thresholds to be set by testing every pairs of cameras. It is not an easy job. This paper proposes the normalized criterion for setting the threshold of epipolar constraint in section III.

### III. THE NORMALIZED EPIPOLAR CONSTRAINT

#### a. The Error on Fundamental Matrix

When the parameters of cameras have been calibrated, then the fundamental matrix is constant. Consequently, the value of Equation (3) is only determined by two pixel coordinates,  $m_i = (u_i, v_i, 1)^T$  and  $m_j = (u_j, v_j, 1)^T$ . Then, a function can be set up as follow,

$$f(m_i, m_j) = m_j^T F m_i \quad (21)$$

It is reasonable to assume that pixel coordinates are disturbed by independent and identically distributed (iid) noises. Let these pixel coordinates be disturbed by iid noises,  $\Delta u_i, \Delta v_i, \Delta u_j, \Delta v_j$ , whose standard deviation are  $\sigma$ . There are some statistical characteristic as follow.

$$\begin{cases} E(u_i) = E(v_i) = E(u_j) = E(v_j) = 0 \\ E(u_i v_i) = E(u_i u_j) = E(u_i v_j) = 0 \\ E(v_i u_j) = E(v_i v_j) = E(u_j v_j) = 0 \\ E(u_i^2) = E(v_i^2) = E(u_j^2) = E(v_j^2) = \sigma^2 \\ E(u_i^2 v_i^2) = E(u_i^2 u_j^2) = E(u_i^2 v_j^2) = \sigma^4 \\ E(v_i^2 u_j^2) = E(v_i^2 v_j^2) = E(u_j^2 v_j^2) = \sigma^4 \end{cases} \quad (22)$$

Let  $\Delta_i = (\Delta u_i, \Delta v_i, 0)^T$ ,  $\Delta_j = (\Delta u_j, \Delta v_j, 0)^T$   $F = \begin{bmatrix} a_1 & a_2 & a_3 \\ a_4 & a_5 & a_6 \\ a_7 & a_8 & a_9 \end{bmatrix}$ . Then The error,  $\Delta f$ , attributed to



the image noise, is calculated as follow.

$$\begin{aligned}\Delta f &= f(u_i + \Delta u_i, v_i + \Delta v_i, u_j + \Delta u_j, v_j + \Delta v_j) - f(u_i, v_i, u_j, v_j) \\ &= m_j^T + \Delta_j^T F m_i + \Delta_i - m_j^T F m_i \\ &= \Delta_j^T F m_i + m_j^T F \Delta_i + \Delta_j^T F \Delta_i\end{aligned}\quad (23)$$

Now this paper calculates some items included in Equation (23) as follow.

$$\begin{aligned}\Delta_j^T F m_i &= \begin{bmatrix} \Delta u_j, \Delta v_j, 0 \end{bmatrix} \begin{bmatrix} a_1 & a_2 & a_3 \\ a_4 & a_5 & a_6 \\ a_7 & a_8 & a_9 \end{bmatrix} \begin{bmatrix} u_i \\ v_i \\ 1 \end{bmatrix} \\ &= a_1 u_i + a_2 v_i + a_3 \Delta u_j + a_4 u_i + a_5 v_i + a_6 \Delta v_j\end{aligned}\quad (24)$$

$$\begin{aligned}m_j^T F \Delta_i &= \begin{bmatrix} u_j, v_j, 1 \end{bmatrix} \begin{bmatrix} a_1 & a_2 & a_3 \\ a_4 & a_5 & a_6 \\ a_7 & a_8 & a_9 \end{bmatrix} \begin{bmatrix} \Delta u_i \\ \Delta v_i \\ 0 \end{bmatrix} \\ &= a_1 u_j + a_4 v_j + a_7 \Delta u_i + a_2 u_j + a_5 v_j + a_8 \Delta v_i\end{aligned}\quad (25)$$

$$\begin{aligned}\Delta_j^T F \Delta_i &= \begin{bmatrix} \Delta u_j, \Delta v_j, 0 \end{bmatrix} \begin{bmatrix} a_1 & a_2 & a_3 \\ a_4 & a_5 & a_6 \\ a_7 & a_8 & a_9 \end{bmatrix} \begin{bmatrix} \Delta u_i \\ \Delta v_i \\ 0 \end{bmatrix} = \begin{bmatrix} \Delta u_j, \Delta v_j, 0 \end{bmatrix} \begin{bmatrix} a_1 \Delta u_i + a_2 \Delta v_i \\ a_4 \Delta u_i + a_5 \Delta v_i \\ a_7 \Delta u_i + a_8 \Delta v_i \end{bmatrix} \\ &= a_1 \Delta u_i \Delta u_j + a_2 \Delta u_j \Delta v_i + a_4 \Delta u_i \Delta v_j + a_5 \Delta v_i \Delta v_j\end{aligned}\quad (26)$$

For clarity, the authors set  $k_1 = a_1 u_j + a_4 v_j + a_7$ ,  $k_2 = a_2 u_j + a_5 v_j + a_8$ ,  $k_3 = a_1 u_i + a_2 v_i + a_3$ , and  $k_4 = a_4 u_i + a_5 v_i + a_6$ . Finally, the error of equation (21) attributed to these noises is as follows.

$$\begin{aligned}\Delta f &= k_1 \Delta u_i + k_2 \Delta v_i + k_3 \Delta u_j + k_4 \Delta v_j \\ &\quad + a_1 \Delta u_i \Delta u_j + a_2 \Delta u_j \Delta v_i + a_4 \Delta u_i \Delta v_j + a_5 \Delta v_i \Delta v_j\end{aligned}\quad (27)$$

According to the equation (22) and the properties of iid noises, the mean of error is as follow.

$$\begin{aligned}E \Delta f &= k_1 E(\Delta u_i) + k_2 E(\Delta v_i) + k_3 E(\Delta u_j) + k_4 E(\Delta v_j) + a_1 E(\Delta u_i \Delta u_j) \\ &\quad + a_2 E(\Delta u_j \Delta v_i) + a_4 E(\Delta u_i \Delta v_j) + a_5 E(\Delta v_i \Delta v_j) = \theta_F = 0\end{aligned}\quad (28)$$

The variance of error can be computed as follow.

$$\text{Var } \Delta f = E \Delta f^2 - E(\Delta f)^2 = E \Delta f^2 - \theta_F = E \Delta f^2\quad (29)$$

There are some items contained in Equation (29) can be calculated as follow

$$E k_1 \cdot \Delta u_i \cdot \Delta f = E k_1^2 \cdot \Delta u_i^2 = k_1^2 \cdot E \Delta u_i^2 = k_1^2 \sigma^2\quad (30)$$

$$E k_2 \cdot \Delta v_i \cdot \Delta f = E k_2^2 \cdot \Delta v_i^2 = k_2^2 \cdot E \Delta v_i^2 = k_2^2 \sigma^2\quad (31)$$

$$E k_3 \cdot \Delta u_j \cdot \Delta f = E k_3^2 \cdot \Delta u_j^2 = k_3^2 \cdot E \Delta u_j^2 = k_3^2 \sigma^2 \quad (32)$$

$$E k_4 \cdot \Delta v_j \cdot \Delta f = E k_4^2 \cdot \Delta v_j^2 = k_4^2 \cdot E \Delta v_j^2 = k_4^2 \sigma^2 \quad (33)$$

$$E a_1 \cdot \Delta u_i \cdot \Delta u_j \cdot \Delta f = E a_1^2 \cdot \Delta u_i^2 \cdot \Delta u_j^2 = a_1^2 \cdot E \Delta u_i^2 \cdot \Delta u_j^2 = a_1^2 \sigma^4 \quad (34)$$

$$E a_2 \cdot \Delta u_j \cdot \Delta v_i \cdot \Delta f = E a_2^2 \cdot \Delta u_j^2 \cdot \Delta v_i^2 = a_2^2 \cdot E \Delta u_j^2 \cdot \Delta v_i^2 = a_2^2 \sigma^4 \quad (35)$$

$$E a_4 \cdot \Delta u_i \cdot \Delta v_j \cdot \Delta f = E a_4^2 \cdot \Delta u_i^2 \cdot \Delta v_j^2 = a_4^2 \cdot E \Delta u_i^2 \cdot \Delta v_j^2 = a_4^2 \sigma^4 \quad (36)$$

$$E a_5 \cdot \Delta v_i \cdot \Delta v_j \cdot \Delta f = E a_5^2 \cdot \Delta v_i^2 \cdot \Delta v_j^2 = a_5^2 \cdot E \Delta v_i^2 \cdot \Delta v_j^2 = a_5^2 \sigma^4 \quad (37)$$

According to Equation (30) ~ (37), the variance of error is as follow.

$$\sigma_F^2 = \text{Var} \Delta f = \sum_{n=1}^4 k_n^2 \sigma^2 + a_1^2 + a_2^2 + a_4^2 + a_5^2 \sigma^4 \quad (38)$$

Additionally, the approximate value of  $\sigma_F^2$  can be achieved by the rules of Propagation Uncertainty as follow [17].

$$\sigma_F^2 \approx \left( \frac{\partial f}{\partial m_i} \right)^2 \sigma^2 + \left( \frac{\partial f}{\partial m_j} \right)^2 \sigma^2 = m_i^T F^T F m_i + m_j^T F^T F m_j \sigma^2 \quad (39)$$

The computational cost of Equation (39) is less than Equation (38). In some case, it is appropriate choice.

#### b. Normalized Method to Set Threshold

As mentioned section 2.3, the parameters of cameras have influence on the values of MP, ED, IA. However,  $\sigma_F^2$  implicates the range of value of Equation (21). Therefore,  $\sigma_F^2$  provides the normalized method to set the threshold of epipolar constraint and eliminate the influence of camera's parameters. The normalized method is described as follow.

$$NE = \frac{|m_j F m_i|}{k \sqrt{\sigma_F^2}} < \varepsilon \quad (40)$$

where  $k$  is a factor of systematic error,  $\varepsilon$  is a threshold. Generally, a value greater than 1 is assigned to  $k$ . If these noises obey Gaussian distribute, it is suitable to set  $\varepsilon = 3$ .

Generally, a multi-ocular system adopts the same cameras and uses the same calibration technique to calibrate all cameras. So, all cameras of the multi-ocular system are similar in the systematic errors and noises. Thus, in a multi-ocular system,  $k$ ,  $\sigma_F$  and  $\varepsilon$  of all cameras are

similar in Equation (40). By the way defined in Formula (40), the threshold of epipolar constraint can be given depended statistic method rather than empirical approach. This paper saves the results of point correspondence of a binocular system by a match matrix, in which if two projections from different cameras satisfy the constraint in Equation (40), the value of corresponding cell will be set 1, otherwise be set 0 (see Fig. 3).

		camera $i$						
		$m_{i1}$	$m_{i2}$	$m_{i3}$	$m_{i4}$	$m_{i5}$	.....	$m_{in}$
camera $j$	$m_{j1}$	1	0	0	0	0	.....	0
	$m_{j2}$	0	1	1	0	0	.....	0
	$m_{j3}$	0	1	1	0	0	.....	0
	$m_{j4}$	0	0	0	0	1	.....	0
	....	0	0	0	0	0	.....	.....
	$m_{jn}$	0	0	0	1	0	.....	0

Figure 3. The match matrix for point correspondence of a binocular system

In Fig. 3, there are ambiguities between the projections  $m_{i2}$ ,  $m_{i3}$ ,  $m_{j2}$  and  $m_{j3}$ . This means these projections and the baseline are coplanar.

What readers should note here is that for an multi-ocular system has  $w$  ( $w \geq 2$ ) cameras, it can

constructs  $d = \frac{1}{2} \binom{2}{w}$  binocular systems, thus the number of match matrix for the multi-ocular system is  $d$ .

#### IV. THE POINT CORRESPONDENCE IN MULTI-OCULAR SYSTEM

##### a. The Analyses of Existing Methods

Binocular system cannot prevent ambiguity happening [13].

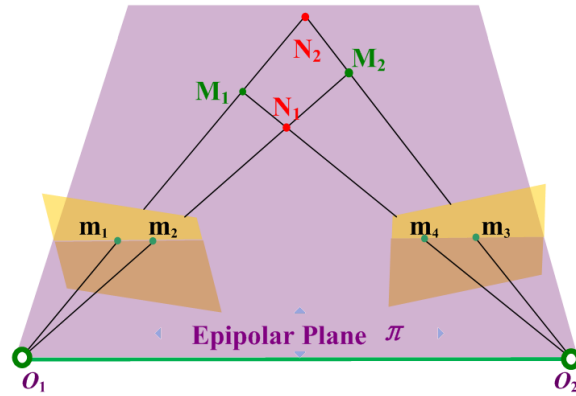


Figure 4. The nature of ambiguity in binocular system

For example, the case depicted in Fig. 4,  $M_1$  and  $M_2$  are in an epipolar plane, the resultant of using  $m_1 \sim m_4$  to reconstruct the 3D-points may be  $M_1$  and  $M_2$  or may be  $N_1$  and  $N_2$ . This phenomenon is called the ambiguity of point correspondence.  $N_1$  and  $N_2$  are named as spurious points by Denton [13]. In fact, the ambiguity arises from projections being on the same epipolar plane, that is to say, the ambiguity of correspondence is inevitable when two 3D-points and the baseline are coplanar.

Thus, the ambiguity can be alleviated by a multi-ocular system whose optical centers are noncollinear. Hartley and Zisserman etc. introduced trifocal tensor, which incorporates geometric relationships of corresponding points in tri-ocular system [14][18]. Some researchers take it as constraint to find corresponding points [19]~[21]. Essentially, trifocal tensor is a trilinear constraint and a generation of fundamental matrix. Namely, trifocal tensor is a generation of traditional epipolar constraint. With the assumption that all 3D-points are visible to all cameras, Amici etc. have proposed a correspondence method in quadri-ocular system. They selected a reference camera, and construct a set of triangles based on the epipolar lines of the other three cameras; then they found corresponding points by finding minimum-area-triangles [15]. These methods can efficiently alleviate the ambiguity of correspondence, but they have two disadvantages. One is that they cannot use the normalized epipolar constraint, and another is the computational complexity attributed to combinatorial problem. The computational complexity is mainly determined by the number of combinations as follows.

$$\frac{1}{2} \binom{k}{w} n^k \quad (41)$$

where  $w \geq 2$  is the number of cameras in an multi-ocular system,  $k \geq 2$  is the number of

projective points used for each verification simultaneously,  $n$  is the number of 3D-points waiting for reconstruction.

Obviously, the computational complexity mainly depends on  $k$  with a given  $n$ . For instance, the computational complexity of Amici's method and trifocal tensor method are  $O(n^4)$  and  $O(n^3)$ . This paper uses uniqueness constraint to reduce the computational complexity by making  $k = 2$ .

#### b. Point Correspondence in Multi-Ocular System

Marr and Poggio put forth the uniqueness constraint that means any two corresponding points are the projections of a unique 3D-point, and the correspondence between them is bidirectional [6]. Therefore, it is reasonable that if  $m_1$  and  $m_2$  are correspondent, and  $m_1$  and  $m_3$  are correspondent, then  $m_2$  and  $m_3$  also are correspondent. This is named as transitivity constraint in this paper. It implicates whether several projective points are corresponding can be verified by whether any two of them are correspondent. Its mathematical expression can be described as follow.

$$\{m_1, m_2\} \wedge \{m_1, m_3\} \Rightarrow \{m_1, m_2, m_3\} \quad (42)$$

In fact, Equation (42) is the way to verify the correspondence in a trinocular system by using the transitivity constraint. Similarly, in a multi-ocular system, which has  $w$  cameras, the correspondence can be verified by the formula described as follows.

$$\{m_1, m_2, \dots, m_w\} \Leftrightarrow \bigwedge_{\substack{i, j=1, \dots, w \\ i \neq j}} \{m_i, m_j\} \quad (43)$$

where  $m_1 \sim m_w$  are the projections of a 3D-point in different cameras.

Based on all achievements above mentioned, we can construct a two-step strategy, which utilizes epipolar constraint to achieve point correspondence in multi-ocular system by normalized threshold and transitivity constraint. Firstly, the normalized epipolar constraint is used in each binocular systems to find some candidates saved in match matrixes for correspondence. And then these candidates are verified by transitive constraint. The procedure of the two-step strategy is as follow.

Step1. Find corresponding points from a pair of cameras with Equation (40), and save the corresponding relationship in a match matrix. The computational complexity of the step is  $O(n^2)$ ,

where  $n$  is the number of 3D-points waiting for reconstruction.

Step2. Repeat Step1 for every pairs of image sensors. Note that there are  $\frac{1}{2} \binom{k}{w}$  match matrixes,

so the computational complexity in the step is  $O n^2$ .

Step3. Use Equation (43) to verify whether three projective points are corresponding based on the three match matrixes. The computational complexity of this step is  $O n$ .

It can be found that, the computational complexity of our strategy for correspondence in multi-ocular system approximately is  $O n^2$ . With the increasing number of 3D-points, the superiority of our two-step strategy will be more remarkable in correspondence problem.

## V. EXPERIMENTS

A quadri-ocular system that has four cameras denoted by I1 ~ I4 and twenty-seven 3D-points are adopted for testing MP, ED and IA method. During experiment, the ideal projective points of these 3D-points are first obtained by equation (1), and then two thousand test projective points of each ideal projective point are generated by iid noises, thirdly the values of these methods are computed with equation (18) ~ (20), finally the standard deviation (STD) of the values are calculated. This paper has introduced some different noises to tested these methods, the results are similar each other. Some results with Gaussian noises are demonstrated as follow (see Fig. 5 ~ Fig. 7).

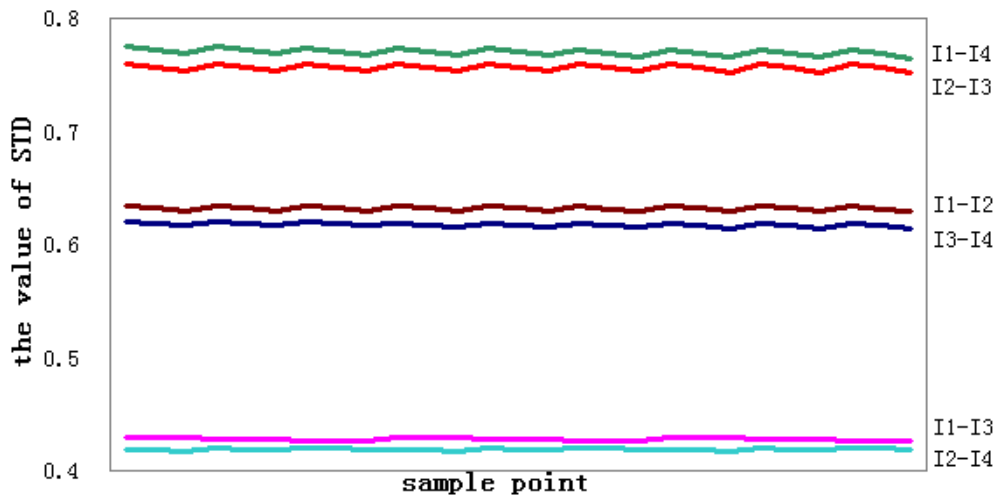


Figure 5. MP method with Gaussian noise  $N(0,1)$ .

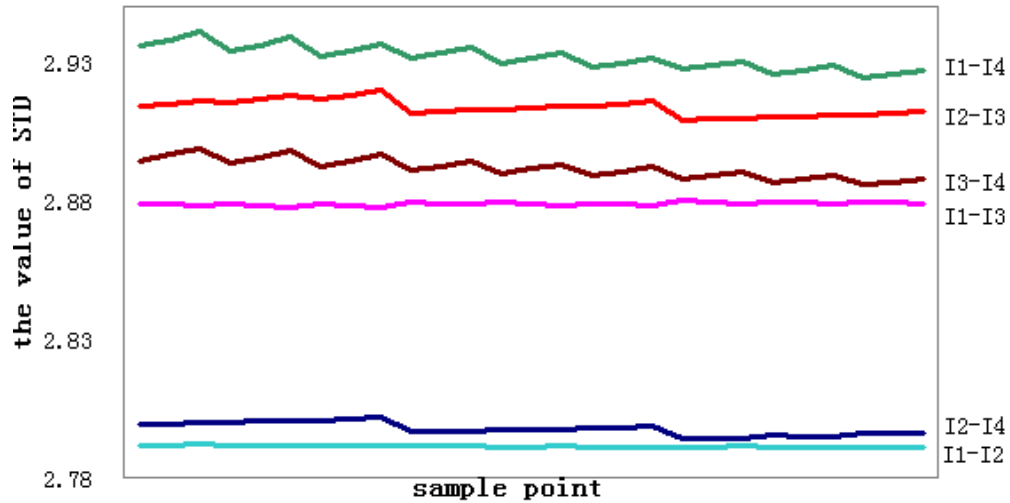
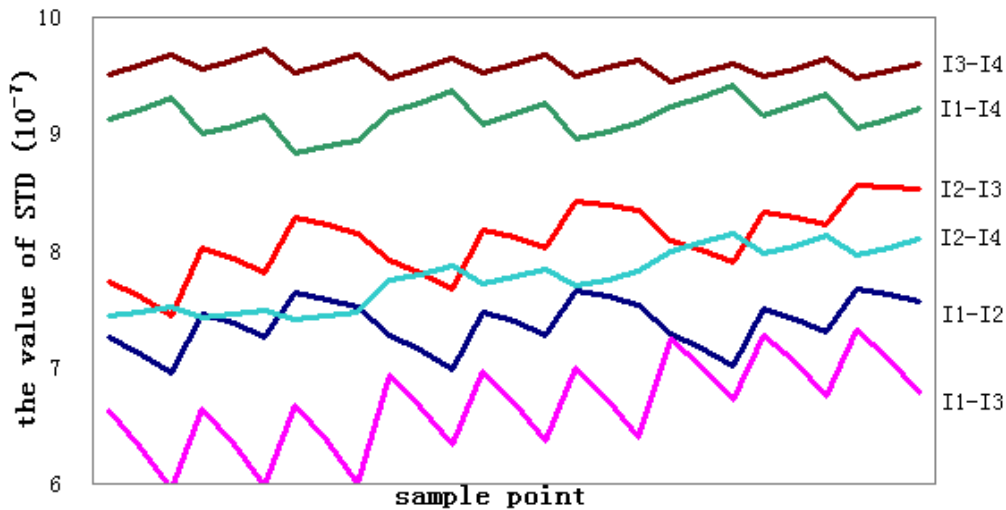
Figure 6. ED method with Gaussian noise  $N(0,1)$ .Figure 7. IA method with Gaussian noise  $N(0,1)$ .

Fig. 5 ~ 7 show that for three methods, every pairs of cameras has different the value of STD, this means every pairs of cameras in the multi-ocular system should be set a specific threshold. Figures also show the STD of MP is rather stable in a certain pair of cameras. This is why the normalized threshold proposed by this paper is based on MP method.

The STD of MP derived from experiment is named as SSD, and the STD obtained by Equation (38) is named as ESD. The similarity of them is evaluated as follows.

$$sim = \left| \frac{SSD - ESD}{SSD} \right| \quad (15)$$

Many experiments shown  $sim < 0.02$ , this means Equation (38) can predict the STD of MP exactly. Therefore, it is feasible to set the normalized threshold of a multi-ocular system by

Equation (40).

The authors of this paper have implemented the two-step strategy in a quadri-ocular system for the spine surgical robot system that is exhibited on Shenzhen High-Tech Fair (see Fig. 8). The practical operation indicates that the speed and robustness of our approach is satisfactory.

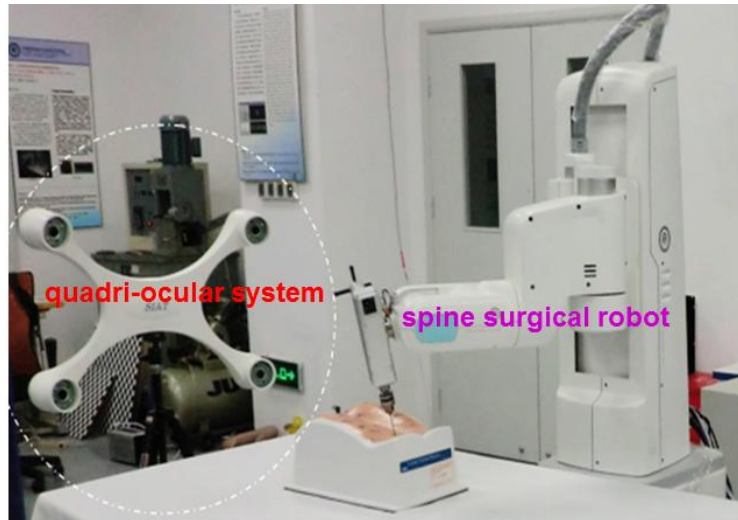


Figure 8. The quadri-ocular system and spine surgical system

## VI. CONCLUSION

This paper proposes a novel two-step strategy using epipolar constraint to implement point correspondence in multi-ocular system by normalized threshold and transitivity constraint. Firstly, the normalized epipolar constraint is used in binocular systems to find some candidates for correspondence. And then these candidates are verified by transitive constraint.

In fact, the normalized threshold is relative to the standard deviation of MP, it provides a statistic method rather than empirical method to set the threshold of epipolar constraint and alleviates the workload to set threshold of a multi-ocular system. The experiment has shown the advantages of normalized epipolar constraint method over MP, ED and IA method.

The transitivity constraint provides a uniform strategy to solve the task of point correspondence in an ocular system regardless of the number of cameras. According to the theoretical analyses, the computation cost of our approach is less than Trifocal tensor method and Amici's method. Therefore, our approach has practical value for point correspondence in multi-ocular systems.



## ACKNOWLEDGMENTS

This work was supported by Guangdong Innovative Research Team Program (No. 201001D0104648280), Shenzhen Sc. & Tech. Research Funds (JC201005280619A), and Guangzhou Nansha Research Funds.

## REFERENCES

- [1] M. Okutomi, T. Kanade, "A multiple-baseline stereo," Computer Vision and Pattern Recognition, Proceedings CVPR ' IEEE Computer Society Conference on, vol, no, Jun 1991, pp.63-69.
- [2] G.L. Gao, D.L. Li, S.H. Shang, "New Method of Cotton Flow Speed Detection Based on Area CCD", Sensor Letters, Volume 8, Number 1, February 2010, pp. 32-39.
- [3] W. Zhang, X. Cao, E. Sung, "A feature-based matching scheme: MPCD and robust matching strategy. Pattern Recognition Letters", 2007, pp. 1222-1231.
- [4] H.C. Longuet-Higgins, "A computer algorithm for reconstructing a scene from two projections", Nature, Vol. 293, Sep 1981, pp. 133-135.
- [5] H. Harlyn Baker, Thomas O. Binford, "Depth from edge and intensity based stereo", Proceedings of the 7th international joint conference on Artificial intelligence, Vancouver, BC, Canada, August, 1981, pp. 631-636.
- [6] D. Marr and T. Poggio., "A Computational Theory of Human Stereo Vision", Proc. Royal Society of London, Vol. 204 of B, 1979, pp. 301-328.
- [7] C.H. Kuo, F.C. Huang, F.C. Yang, "Development of active IR-based surgical marker tracking and positioning systems", Systems, Man and Cybernetics, IEEE International Conference on , vol.3, no., Oct. 2005, pp. 2443-2448.
- [8] S.S. Chawathe, "Marker-Based Localizing for Indoor Navigation", IEEE Intelligent Transportation Systems Conference, 2007, vol., no., Sept 2007, pp. 885-890,.
- [9] P. Zhou, Y. Liu, Y.T. Wang, "Multiple infrared markers based real-time stereo vision positioning system for surgical navigation", Instrumentation and Measurement Technology Conference, 2009.
- [10] M. Galo, C.L. Tozzi, "The concept of matching parallelepiped and its use in the

correspondence problem”, Image Processing, International Conference on, vol.4, no, 1999, pp.410-414.

[11] Z.Y. Zhang, “Determining the epipolar geometry and its uncertainty: A review”, International Journal of Computer Vision, Vol.27, No.2, 1998, pp. 161-198.

[12] A. M. M. Muijtjens, J. M. A. Roos, T. Arts, A. Hasman, R. S. Reneman, “Simultaneous estimation of stereo correspondence and camera geometry from marker tracks”, Computers in Cardiology, vol., no., Sep 1995, pp. 577-580,

[13] J. A. Denton, J. R. Beveridge, “An algorithm for projective point matching in the presence of spurious points”, Pattern Recognition, Volume 40, Issue 2, February 2007, pp. 586-595.

[14] R.I. Hartley, “Lines and Points in Three Views and the Trifocal Tensor”, International Journal of Computer Vision 1997, pp. 125-140.

[15] S. De Amici, A. Sanna, F. Lamberti, B. Pralio, “A Wii remote-based infrared-optical tracking system”, Entertainment Computing, Volume 1, Issues 3-4, December 2010, pp. 119-124.

[16] F.Z. Wu, “Mathematical Methods in Computer Vision”, Science Press, Beijing, China, 2008.

[17] Fornasini, Paolo, “The uncertainty in physical measurements: an introduction to data analysis in the physics laboratory”, Springer, Germany, 2008.

[18] P. Torr and A. Zisserman. “Robust Parameterization and Computation of the Trifocal Tensor”, Image and Vision Computing, 1997, pp. 591-607.

[19] J. Zhang, F.H. Shi, Y.C. Liu, “Motion Segmentation by Multibody Trifocal Tensor Using Line Correspondence”, Pattern Recognition. ICPR 2006. 18th International Conference on , vol.1, no., 2006, pp. 599-602.

[20] T. Molinier, D. Fofi, F. Meriaudeau, and R. Seulin, “Trifocal tensor as a tool for modeling an imperceptible structured light sensor”, J. Opt. Technol, 2007, pp. 282-287.

[21] R. Vida, R. Hartley, “Three-View Multibody Structure from Motion”, Pattern Analysis and Machine Intelligence, IEEE Transactions on, vol.30, no.2, Feb. 2008, pp. 214-227.